DOI: 10.21917/ijivp.2022.0375

HYPERSPECTRAL AND MULTISPECTRAL IMAGE FUSION USING FULLY CONSTRAINED NONLINEAR COUPLED NONNEGATIVE MATRIX FACTORIZATION

K. Priya and K.K. Rajkumar
Department of Information Technology, Kannur University, India

Abstract

Hyperspectral images (HSI) have a wide range of spectral information compared to conventional images. This rich spectral information leads to store more information about the image. Even though the hyperspectral images have multiple spectrum bands that makes narrow division of each spectral band in the image. This narrow band division reduces the spatial quality of HSI and hence it necessitates the improvement of the spatial quality of the hyperspectral image. One of the most emerging methods to improve or enhance the hyperspectral image quality is the HS-MS image fusion. Most of the existing image fusion methods neglects the nonlinear data associated with the image. To overcome this limitation, we proposed a nonlinear unmixing-based fusion model, namely Fully Constrained Nonlinear-CNMF (FCN-CNMF) by consider the nonlinearity data associated with the image. To improve the performance of our nonlinear unmixing-based fusion method, we imposed certain constraints on both spectral and spatial data. The constraints include minimum volume simplex with spectral data and total variance and sparsity with spatial data to enhance the quality of the image. We applied all these constraints to both hyperspectral and multispectral images and then fused these data to obtain the final high-quality image. The fused image's quality is measured using five standard quality measures on four benchmark datasets and found that the proposed method shows superiority over all baseline methods.

Keywords:

Hyperspectral Image, Nonlinearity, Spectral Unmixing, Spectral Image Fusion

1. INTRODUCTION

. Hyperspectral (HS) images are enriched with high spectral information than conventional images. This property makes the energy collected by hyperspectral sensors are divided into several narrow wavelength bands. However, this narrow partitioning reduces the amount of energy received by each band [1]. Due to these characteristics, many kinds of noise are easily influenced by the HS image which may cause a reduction in the spatial quality of the hyperspectral image. So, it is necessary to enhance the spatial quality of the HS image [2]. One popular method is the fusion between multispectral (MS) image and hyperspectral (HS) image. This fusion helps to reconstruct the hyperspectral image that possesses high spectral and spatial resolution. The existing literature also reveals that spectral unmixing (SU) based fusion is one of the main approaches for the enhancement of hyperspectral images [3].

In the SU-based HS-MS data fusion approach, the high-spatial data of MS image with high-spectral data of HS image are fused together [4]. The CNMF based fusion is a trending HS-MS fusion approach, but the nonlinearity factor is still a problem in the performance of the LMM based CNMF method [5]. The nonlinearity factors also called the outlier data, such as low illumination pixels that are avoided during the LMM process. These nonlinear outlier data may effects many important factors like object boundary, and image topography, play a prominent role in enhancing hyperspectral images [6]. These Ignored outlier data pay considerable attention during the reconstruction of hyperspectral image [7].

In this work, we proposed a fully constrained nonlinear - CNMF (FCN-CNMF) algorithm. The main contribution of this algorithm is enhance the visual quality of the reconstructed HSI image without any spatial or spectral degradation and also by considering the nonlinear data in the image. This algorithm fuses the endmember data from the hyperspectral image with abundance data from the multispectral image by including the outlier term. Thus, produce a highly stable and robust fusion algorithm, namely FCN-CNMF. Finally, this fusion algorithm produces a high fidelity reconstructed hyperspectral image close to a high-resolution referenced image. This proposed FCN-CNMF algorithm is experimented on various hyperspectral datasets [8] and compared with many existing algorithms to determine the quality of fusion results.

The following sections are arranged as follows: In section 2 includes the detailed literature review related to spectral unmixing-based fusion and identifies the proper research gap in unmixing-based fusion using a linear mixing model. The section 3 formulated the proposed model, followed by the explanation of the FCN-CNMF algorithm is given in section 4. The section 5 implements the proposed model and section 6 gives the experiments and performance analysis. Finally, section 7 concludes this paper with future scope.

2. LITERATURE REVIEW

Existing literature reveals that spectral unmixing-based fusion is one of the promising approaches for enhancement of hyperspectral images. Yokoya et al. [9] introduced a CNMF method that works on the principle of Linear Mixing Model (LMM). CNMF uses a straightforward approach for unmixing and fusion processes and its mathematical formulation as well as the implementation are not complex compared to the existing fusion methods. Finally, this method optimizes the solution with minimum residual errors and reconstructs the high-fidelity hyperspectral images. The enhancement of the LR-HSI image using this CNMF unmixing-based fusion method is shown in Fig.1.

Simoes et al. [10] introduced a method for hyperspectral image enhancement is termed as HySure. HySure method built a model that preserves the edges between the objects during the unmixing-based data fusion. This method uses a constraint called Vector Total Variation regularizer that preserves the edges and

promotes piecewise smoothness to the spatial quality of the image.

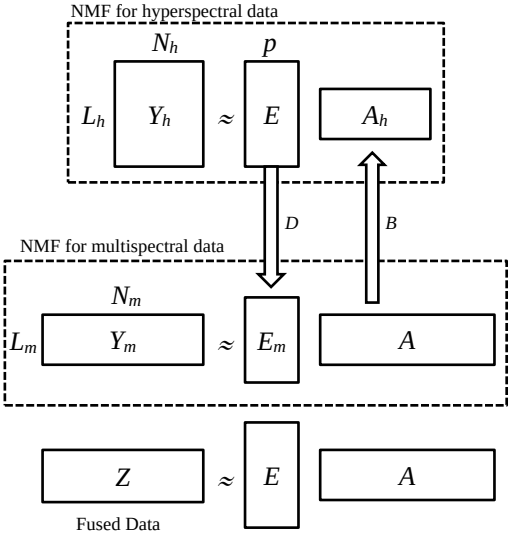

Fig.1. Illustration of CNMF unmixing for HSI and MSI

Lin et al. [11] introduced a CO-CNMF method. This method formulates the problem by incorporating sparsity and SSD regularizer. The SSD regularizer extract high-quality spectral data from the images and promotes sparsity by using l1-norm regularization. This regularizer helps to upgrade the performance of the existing CNMF method. However, some performance degradation may occur in this algorithm at high noise level.

Yang et al. [12] introduced TVSR regularizations CNMF method called TVSR-CNMF. The TV regularizer is added to the abundance matrix to ensure the images spatial smoothness. Similarly, a signature-based regularizer is also added to the endmember matrix for extracting high-quality spectral data, thus helps to reconstruct good hyperspectral images.

Borsoi et al. [13] introduced a FuVar algorithm that aims to deal with the spectral variability among the images. For introducing this spectral signature variability during fusion, a Generalized Linear Mixing Model (GLMM) is developed that uses a scaling factor for each spectral band of the hyperspectral image individually. In this method hyperspectral images are divided into several sub-image and identifies the spectral variability in the sub-images for each spectral band separately. Then applied a scaling factor based on spectral variability. Finally, combine each sub-images to obtain high quality fused image. However, this method creates difficulty in obtaining an optimized solution due to the complex spectral variability.

Yang et al. [14] also introduced a sparsity, and proximal minimum-volume (pmv) regularized CNMF named as SPR-CNMF. The pmv regularizer controls and minimizes the distance between selected endmembers and the center of mass to reduce the computational complexity. Therefore, SPR-CNF with simplex minimum volume concepts improves the fusion performance by controlling the loss of cubic structural information.

From these reviews of the recent unmixing fusion models, it is identified that the CNMF method is based on a LMM which does not consider the nonlinearity factors of the pixels in the image. Therefore, in our proposed work, we modify the CNMF by adding an additive term for considering the nonlinear data such as low-resolution pixel that avoided during LMM process. Thus, improving the performance the fusion algorithms compared to the existing methods [15].

3. PROBLEM FORMULATION

Let $Y_h \in \mathbb{R}^{L_h \times N_h}$ and $Y_m \in \mathbb{R}^{L_m \times N_m}$ be an observed LR-HSI and HR-MSI with L_h, L_m bands and N_m, N_h pixels. Then fuse the band L_h from Y_h and N_m pixels from Y_m to yield the desired high spectral and spatial resolution hyperspectral image, $Z \in \mathbb{R}^{L_h \times N_m}$ [16].

$$Z = EA \tag{1}$$

Then, Y_h and Y_m can be represented as,

$$Y_m \approx DZ + R_m \tag{2}$$

$$Y_h \approx ZB + R_h \tag{3}$$

where $B \in \mathbb{R}^{N_m \times N_h}$ is used to blur the spatial quality of Z to obtain Y_h. $D \in \mathbb{R}^{L_m \times L_h}$ is used to spectral downsampling of Z to obtain Y_m. In general, the matrix R_m and R_h denotes a residual noise, are assumed as zero-mean Gaussian noises. But in this proposed method, the residual term R_m and R_h are considered as a nonnegative matrix to accounts for the nonlinear factors [17].

After unmixing process of both Y_h and Y_m using NMF, fuse the end member E and abundance A by using the CNMF algorithm. That means, CNMF work by combine two NMF algorithms as a product of E and A [19]. From the Eq.(1)-Eq.(3), the minimization functions of NMF unmixing for Y_h and Y_m are defined as,

$$\left\|Y_h - EA_h\right\|_F^2 \text{ and } \left\|Y_m - E_m A\right\|_F^2 \tag{4}$$

where $\left\|\cdot\right\|_F^2$ denotes the Frobenius norm, which minimizes the cost function in hyperspectral unmixing [17]. Then, the objective function for CNMF can be defined as:

$$CNMF\left(E,A\right) = \left\|Y_h - EA_h\right\|_F^2 + \left\|Y_m - E_m A\right\|_F^2 \; s.t.\; E, A \geq 0 \tag{5}$$

The CNMF method is not a well-posed problem. A well-posed problem is one that exists a unique solution to a given set of selected data for providing a stable solution to the problems. A problem that does not satisfy these properties of well-posedness is called an ill-posed problem. The CNMF method does not exist a unique solution and stability to a given set of data. This ill-posedness problem of CNMF can be solved by adding some constraints terms into spectral and spatial data [18].

4. FULLY CONSTRAINED NONLINEAR CNMF METHOD

The standard LMM model does not consider the low contrast pixels in the image. But in the case of a real-time image, it is necessary to consider these low-resolution pixels to improve the image visual effect. So, in this model, we including an additional residual term as R with LMM, which accounts for all possible nonlinear effects in the image. This residual term R is measured as the deviation between the original and estimated data [15]. Therefore, the NMF unmixing for Y_h and Y_m, are defined as,

$$\left\|Y_h - \left(EA_h + R_h\right)\right\|_F^2 \tag{6}$$

$$\left\|Y_m-\left(E_mA+R_m\right)\right\|_F^2 \quad (7)$$

Then the CNMF representation for Eq.(6) and Eq.(7) can be redefined as,

$$CNMF\left(E,A,R\right)=\left\|Y_h-\left(EA_h+R_h\right)\right\|_F^2+\left\|Y_m-\left(E_mA+R_m\right)\right\|_F^2 \quad (8)$$

The parameter R controls the ill-posed problem of CNMF and thus produces high fidelity reconstructed image.

In this model, we also enhance the quality of extracted data by adding all available constraints from the literature that affect both the geometrical and statistical data of the image. So, the nonlinear CNMF unmixing for Y_h and Y_m, in Eq.(8) is defined by imposing all essential constraints such as total variation, sparsity, and signature-based minimum volume. Therefore, to reconstruct the image, $Z = EA$, the objective function of the FCN-CNMF method will be as follows:

$$\min CNMF\left(E,A,R\right)+\alpha\varnothing_{MV}\left(E\right)+\beta\varnothing_{TV}\left(A\right)+\lambda\varnothing_{spa}\left(A\right)$$
$$s.t.\ E,A\geq 0 \quad (9)$$

where $CNMF(E,A,R)$ is unconstrained CNMF method, $\alpha>0$ and $\beta>0$ and $\lambda>0$ are the parameters to control the constraints and these constraints are calculated as:

$$\varnothing_{MV}\left(E\right)=\sum_{i=1}^{p}\sum_{j=i+1}^{p}\left\|e_i-e_j\right\|_2^2 \quad (10)$$

$$\varnothing_{spa}\left(A\right)=\sum_{i,j=1}^{p,N}a_{i,j}^{0.5} \quad (11)$$

$$\varnothing_{TV}\left(A\right)=\left\|H_h\tilde{A}\right\|_1+\left\|H_v\tilde{A}\right\|_1 \quad (12)$$

where, $\varnothing_{MV}(E)$, is a minimum volume regularizer that reduce the volume of the simplex in hyperspectral imagery thus helps to estimate high-fidelity spectral signature. $\varnothing_{spa}(A)$, reflects the sparsity that means the amount of zero or null values in abundance $\varnothing_{TV}(A)$, solve the variation between the adjacent pixels and avoid all possible lumps in the spectral signature of the endmember to provide smoothness to the image [20].

5. IMPLEMENTATION

The proposed FCN-CNMF algorithm is implemented by alternatively solving each term (E,A,R) from the LR-HSI and HR-MSI with the constraints until a minimum optimization solution is obtained. At first, unmix the endmembers, abundance, and outlier data of LR-HSI are updated by the multiplication iteration model [20] as follows,

$$R_h^{k+1}=R_h o\left[\frac{Y_h}{E^kA_h^k+\lambda R_h diag\left[\left\|r_{h1}\right\|_1,...,\left\|r_{h1}\right\|_1\right]^{-1}}\right] \quad (13)$$

$$A_h^{k+1}=A_h o\frac{\left(E^k\right)^T\left(Y-R_h^k\right)+\tilde{S}\cdot\tilde{Y}}{\left(E^k\right)^T\left(E^kA_h\right)+\tilde{S}\cdot Y}+\lambda\varnothing_{TV}\left(A_h\right)+\gamma\varnothing_{spa}\left(A_h\right) \quad (14)$$

$$E^{k+1}=Eo\frac{\left(Y_h-R_h^k\right)\left(A_h^k\right)^T}{EA_h^k\left(A_h^k\right)^T}+\alpha\varnothing_{MV}\left(E\right) \quad (15)$$

Similarly, the multiplication iteration model is used to update the endmembers, abundance, and outlier data of HR-MSI as follows,

$$R_m^{k+1}=R_m o\left[\frac{Y_m}{E_m^kA^k+\lambda R_m diag\left[\left\|r_{m1}\right\|_1,...,\left\|r_{m1}\right\|_1\right]^{-1}}\right] \quad (16)$$

$$A^{k+1}=A o\frac{\left(E_m^k\right)^T\left(Y_m-R_m^k\right)+\tilde{S}\cdot\tilde{Y}}{\left(E_m^k\right)^T\left(E_m^kA\right)+\tilde{S}\cdot Y}+\lambda\varnothing_{TV}\left(A\right)+\gamma\varnothing_{spa}\left(A\right) \quad (17)$$

$$E_m^{k+1}=E_m o\frac{\left(Y_m-R_m^k\right)\left(A^k\right)^T}{EA_m^k\left(A^k\right)^T}+\alpha\varnothing_{MV}\left(E_m\right) \quad (18)$$

where the number of iterations is denoted as k. At first unmix, the image Y into E, A and R. The algorithm starts with these initial value as (R^0, A^0, E^0), then proceed in the order as (R^k, A^k, E^k) $\rightarrow$(R^{k+1}, A^k, E^k)$\rightarrow$(R^{k+1}, A^{k+1}, E^k)$\rightarrow$ (R^{k+1}, A^{k+1}, E^{k+1}) so on. These steps are repeated until it meets the stopping condition and are represented as follows.

$$A^{k+1}=\min_{E,A,R}CNMF\left(E_m^k,A,R_m^k\right)+\lambda\varnothing_{TV}\left(A\right)+\gamma\varnothing_{spa}\left(A\right) \quad (19)$$

$$A^{k+1}=\min_{E,A,R}CNMF\left(E,A_h^k,R_h^k\right)+\alpha\varnothing_{MV}\left(E\right) \quad (20)$$

This iterative equation helps to extract high fidelity end member E from LR-HSI, abundance matrix A from HR-MSI. Then fuse these data to produce $\hat{Z}$ as follows,

$$\hat{Z}=EA \quad (21)$$

The reconstructed image $\hat{Z}$ contain spectral and spatial information almost similar to the ground truth image. Algorithm 1, gives the summary of the proposed FCN-CNMF algorithm.

6. EXPERIMENTS AND PERFORMANCE ANALYSIS

The proposed work is implemented in in Python (Spyder) 3.7 platform and the performance of the unmixing-based fusion algorithm FCN-CNMF is evaluated using some standard quality measures on four different public datasets. On evaluation, it is found that our method produces high-fidelity reconstructed image. Finally, the superiority and strength of our method is evaluated by comparing the experiment results with existing methods namely CNMF [9], HySure [10], CO-CNMF [11], TVSR-CNMF [12], and FuVar [13]. The results obtained in all these methods are compared with the proposed FCN-CNMF method and found that our FCN-CNMF method have better fusion output.

6.1 DATASET

We use four real datasets: Washington DC mall, Bostwana, Pavia University, Indian Pines with spectral band 191, 145, 103, and 192 with 400 to 2500 nm spectral range respectively. We crop all datasets with 240×240-pixel size to make algorithm faster [21].

The Y_h is created by blurring the spatial quality of the image Z with a blur factor $\omega = 4$ in horizontal and vertical directions [22]. The Y_m was produced corresponding to Landsat 7 TM bands with

7 spectral bands, where each spectral band covering particular range between 450 - 2350 nm regions, respectively [23].

Algorithm 1: FCN-CNMF algorithm

Input: LR-HSI → Y_h; HR-MSI → Y_m

Initialize: k=0 and (R^0, A^0, E^0)

Step 1: First, unmix Y_h as Eq.(6) using NMF method

Optimize E, A_h and R_h as in Eq.(13)-Eq.(15).

Step 2: Subsequently, unmix Y_m as Eq.(7) using NMF method

Optimize E_m, A and R_m as in Eq.(16), Eq.(17) and Eq.(18)

Step 3: Repeat steps 1 and 2 until reached the stopping condition.

Step 4: Reconstruct Z by observing E from LR-HSI and A from HR-MSI: $Z = EA$

Output: The image Z with high spatial-spectral dimension.

6.2 QUALITY METRICS

The measure the performance of FCN-CNMF algorithm is measured by using following quality metrics [8].

- *Spectral Angle Mapper (SAM)* identifies the spectral difference between the images as follows:

$$SAM\left(E,\hat{E}\right)=\frac{1}{n}\sum_{j=1}^{n}\arccos\left[\frac{E_j^T\cdot\hat{E}_J}{\left\|E_j\right\|_2\cdot\left\|\hat{E}_J\right\|_2}\right] \tag{13}$$

- *Signal-to-Reconstruction Error (SRE)* measures the quality of the FCN-CNMF algorithm as follows:

$$SRE=10\log_{10}\left(\frac{\frac{1}{n}\sum_{i=1}^{n}\left\|\hat{A}_i\right\|_2^2}{\frac{1}{n}\sum_{i=1}^{n}\left\|\hat{A}_i-A_i\right\|_2^2}\right) \tag{14}$$

- *Root-Mean-Square Error (RMSE)* value is measured as:

$$RMSE\left(\hat{A},A\right)=\frac{1}{\lambda_h n_m}\left\|A-\hat{A}\right\|_F^2 \tag{15}$$

- *Peak Signal to Noise Ratio (PSNR)* measures the quality of spatial data in lth band is defined as:

$$RMSE\left(\hat{A},A\right)=\frac{1}{\lambda_h}\sum_{l=1}^{\lambda_h}PSNR_l \tag{16}$$

where $PSNR_l$ measures the spatial quality in the l^{th} spectral band is defined as:

$$PSNR_l=10\log_{10}\left(\frac{\max\left(A^l\right)^2}{\left\|\hat{A}^l-A^l\right\|/P}\right) \tag{17}$$

- *Universal Image Quality Index (UIQI)* measure the structural similarity between the images by calculated as:

$$Q\left(A^l,\hat{A}^l\right)=\frac{\sigma_{A^l\hat{A}^l}}{\sigma_{A^l}\sigma_{\hat{A}^l}}\frac{2\mu_{A^l}\mu_{\hat{A}^l}}{\mu_{A^l}^2+\mu_{\hat{A}^l}^2}\frac{2\sigma_{A^l}\sigma_{\hat{A}^l}}{\sigma_{A^l}^2+\sigma_{\hat{A}^l}^2} \tag{18}$$

$$UIQI\left(A^l,\hat{A}^l\right)=\frac{1}{\lambda_h}\sum_{l=1}^{\lambda_h}Q\left(A^l,\hat{A}^l\right) \tag{19}$$

If the value of $UIQI\left(A^l,\hat{A}^l\right)$ = 1, that means both images are similar [17].

6.3 PERFORMANCE ANALYSIS OF FCN-CNMF FUSION ALGORITHM

The FCN-CNMF algorithm aims to improve both spectral and spatial data by incorporating the nonlinear factor also in the hyperspectral image. So, this proposed algorithm enhances the spatial quality of LR-HSI images.

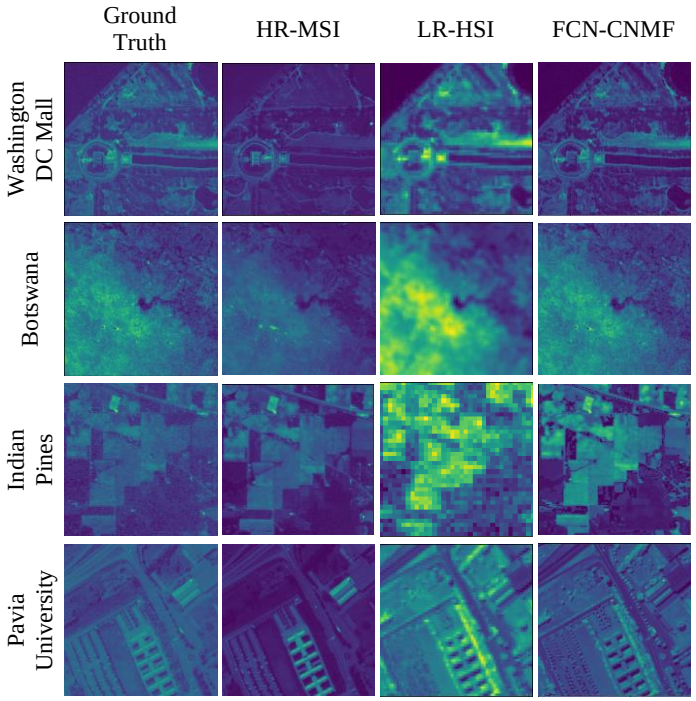

Fig.2. Representation of the ground truth, HR-MSI, LR-HSI, and our FCN-CNMF algorithm images of four datasets

Finally, the proposed FCN-CNMF algorithm fuses these extracted data without any data distortion. The Fig.2 shows output of the FCN-CNMF methods on four different datasets along with its HR-MSI, LR-HSI image. The Fig.2 shows that the FCN-CNMF algorithm gives a better visual effect by enhancing the quality of the images on the above four datasets. The Fig.3 shows the performance of all fusion methods.

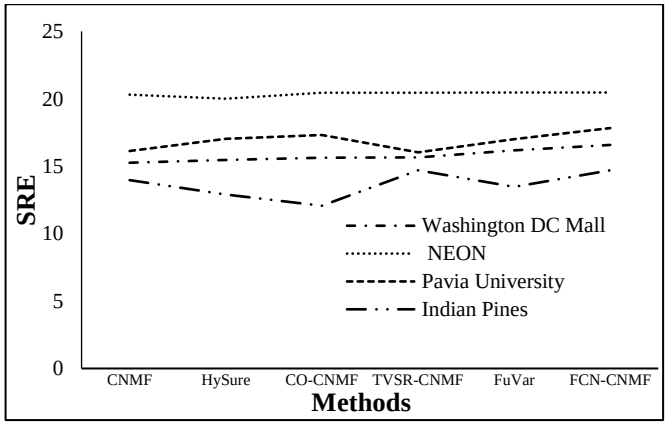

(a) SRE

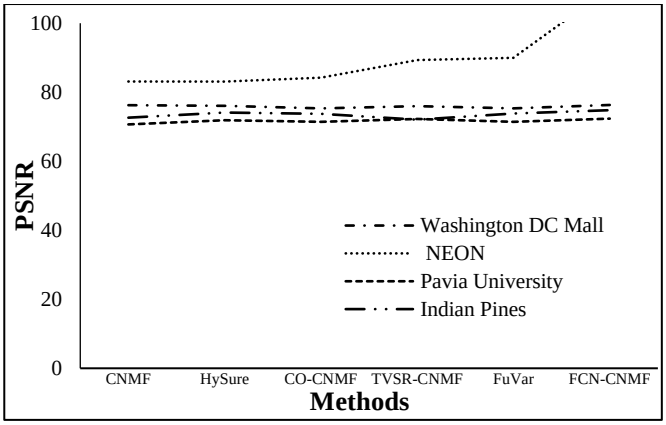

(b) PSNR

Fig.3. Performance representation of all comparison algorithms

Table.1. Quality measures of FCN-CNMF with other algorithm on four Datasets

Dataset	Method	CNMF	HySure	CO-CNMF	TVSR-CNMF	FuVar	FCN-CNMF
Washington DC Mall	SAM	1.01	0.99	0.74	0.74	0.76	0.65
	RMSE	8.57	7.50	7.41	7.43	0.01	0.005
	SRE	15.26	15.46	15.64	15.66	16.17	18.58
	PSNR	76.23	76.02	75.35	76.01	75.33	80.31
	UIQI	0.81	0.89	0.82	0.90	0.91	0.95
Botswana	SAM	0.58	0.67	0.53	0.82	0.50	0.40
	RMSE	5.16	5.18	4.57	4.58	4.58	3.15
	SRE	20.33	20.11	20.76	20.56	21.47	22.47
	PSNR	82.11	84.09	85.23	89.32	91.01	110.14
	UIQI	0.78	0.84	0.67	0.79	0.89	0.96
Pavia University	SAM	0.47	0.34	0.39	0.31	0.30	0.27
	RMSE	1.01	1.21	0.95	1.02	1.08	0.91
	SRE	16.83	17.05	17.39	18.03	18.01	19.83
	PSNR	70.84	72.67	71.23	73.30	73.40	75.35
	UIQI	0.83	0.81	0.93	0.92	0.94	0.96
Indian Pines	SAM	0.005	0.038	0.002	0.004	0.003	0.001
	RMSE	0.021	0.024	0.070	0.07	0.12	0.01
	SRE	13.18	12.98	12.77	14.76	14.48	15.70
	PSNR	76.61	75.11	76.71	77.04	77.85	78.80
	UIQI	0.91	0.89	0.94	0.92	0.95	0.97

Finally, the performance of this FCN-CNMF algorithm is evaluated against the various baseline algorithms using standard quality measures and the results obtained by these methods on four different datasets are shown in Table.1. This result indicates that the FCN-CNMF algorithm is superior to all other baseline fusion methods. The lower SAM and higher PSNR value indicate that the good spectral and spatial quality of reconstructed image. Similarly, the higher value of SRE, UIQI and low value of RMSE shows the better performance of the fusion algorithm during the reconstruction process.

7. CONCLUSION

In this paper, proposed an FCN-CNMF to enhance the LR-HSI by considering the outlier data in the image known as nonlinearity. As a result, this proposed algorithm produces a high-fidelity reconstructed image similar to the referenced image and lowers the algorithm complexity and computational time compared to other fusion algorithms. From this comparison, our FCN-CNMF method shows better performance compared to all other baseline methods. In future work, further improve the accuracy of unmixing performance by introducing more constraints into endmembers and the abundance of the hyperspectral images.

REFERENCES

[1] Ting Xu, Ting Zhu Huang, Liang Jian Deng, XiLe Zhao and Jie Huang, "Hyperspectral Image Superresolution using Unidirectional Total Variation with Tucker Decomposition", *IEEE Journal of Selected Topics in Applied Earth Observations and Remote Sensing*, Vol. 13, pp. 4381-4398, 2020.

[2] Renwei Dian, Shutao Li, Leyuan Fang and Qi Wei. "Multispectral and Hyperspectral Image Fusion with Spatial-Spectral Sparse Representation", *Information Fusion*, Vol. 49, pp. 262-270, 2019.

[3] Naoto Yokoya, Claas Grohnfeldt and Jocelyn Chanussot. "Hyperspectral and Multispectral Data Fusion: A Comparative Review of the Recent Literature", *IEEE Geoscience and Remote Sensing Magazine*, Vol. 5, No. 2, pp. 29-56, 2017.

[4] Renwei Dian, Shutao Li, Leyuan Fang, Ting Lu and Jose M. Bioucas-Dias, "Nonlocal Sparse Tensor Factorization for Semiblind Hyperspectral and Multispectral Image Fusion", *IEEE Transactions on Cybernetics*, Vol. 50, No. 10, pp. 4469-4480, 2019.

[5] Xuelong Li, Yue Yuan and Qi Wang, "Hyperspectral and Multispectral Image Fusion via Nonlocal Low-Rank Tensor Approximation and Sparse Representation", *IEEE Transactions on Geoscience and Remote Sensing*, Vol. 59, No. 1, pp. 550-562, 2020.

[6] Danfeng Hong, Naoto Yokoya, Jocelyn Chanussot and Xiao Xiang Zhu, "An Augmented Linear Mixing Model to Address Spectral Variability for Hyperspectral Unmixing", *IEEE Transactions on Image Processing*, Vol. 28, No. 4, pp. 1923-1938, 2019.

[7] Danfeng Hong, Naoto Yokoya, Jocelyn Chanussot and Xiao Xiang Zhu, "Learning a Low Coherence Dictionary to Address Spectral Variability for Hyperspectral Unmixing", *Proceedings of IEEE International Conference on Image Processing*, pp. 1-13, 2017.

[8] Xinyu Zhou, Ye Zhang, Junping Zhang and Shaoqi Shi, "Alternating Direction Iterative Nonnegative Matrix Factorization Unmixing for Multispectral and Hyperspectral Data Fusion", *IEEE Journal of Selected Topics in Applied Earth Observations and Remote Sensing*, Vol. 13, pp. 5223-5232, 2020.

[9] N. Yokoya, T. Yairi and A. Iwasaki, "Coupled Nonnegative Matrix Factorization Unmixing for Hyperspectral and Multispectral Data Fusion", *IEEE Transactions on Geoscience and Remote Sensing*, Vol. 50, No. 2, pp. 528-537, 2012.

[10] M. Simoes, J. Bioucas Dias, L.B. Almeida and J. Chanussot, "A Convex Formulation for Hyperspectral Image Superresolution via Subspacebased Regularization", *IEEE Transactions on Geoscience and Remote Sensing*, Vol. 53, No. 6, pp. 3373-3380, 2015.

[11] C.H. Lin, F. Ma, C.Y. Chi and C.H. Hsieh, "A Convex Optimization-Based Coupled Nonnegative Matrix Factorization Algorithm for Hyperspectral and Multispectral Data Fusion", *IEEE Transactions on Geoscience and Remote Sensing*, Vol. 56, No. 3, pp. 1652-1667, 2018.

[12] Feixia Yang, Fei Ma, Ziliang Ping and Guixian Xu, "Total Variation and Signature-Based Regularizations on Coupled Nonnegative Matrix Factorization for Data Fusion", *IEEE Access*, Vol. 7, pp. 1-13, 2019.

[13] Ricardo Augusto Borsoi, Tales Imbiriba and Jose Carlos Moreira Bermudez, "Super-Resolution for Hyperspectral and Multispectral Image Fusion Accounting for Seasonal Spectral Variability", *IEEE Transactions on Image Processing*, Vol. 19, pp. 116-127, 2019.

[14] Feixia Yang, Ziliang Ping, Fei Ma and Yanwei Wang, "Fusion of Hyperspectral and Multispectral Images With Sparse and Proximal Regularization", *IEEE Access*, Vol. 7, pp. 891-899, 2019.

[15] Cedric Fevotte and Nicolas Dobigeon, "Nonlinear Hyperspectral Unmixing with Robust Nonnegative Matrix Factorization", *IEEE Transactions on Image Processing*, Vol. 24, No. 12, pp. 1-16, 2015.

[16] Fei Ma, Feixia Yang, Ziliang Ping and Wenqin Wang, "Joint Spatial-Spectral Smoothing in a Minimum-Volume Simplex for Hyperspectral Image Super-Resolution", *Applied Sciences*, Vol. 10, No. 1, pp. 237-256, 2019.

[17] D. Hong, N. Yokoya, J. Chanussot and X. Zhu, "An Augmented Linear Mixing Model to Address Spectral Varialbilty for Hyperspectral Unmixing, Geography", *IEEE Transactions on Image Processing*, Vol. 54, No. 3, pp. 1-17, 2018.

[18] Naoto Yokoya, Takehisa Yairi and Akira Iwasaki, "Coupled Nonnegative Matrix Factorization Unmixing for Hyperspectral and Multispectral Data Fusion", *IEEE Transactions on Geoscience and Remote Sensing*, Vol. 50, No. 2, pp. 528-537, 2012.

[19] Li Sun, Kang Zhao and Ziwen Liu, "Enhancing Hyperspectral Unmixing With Two-Stage Multiplicative Update Nonnegative Matrix Factorization", *IEEE Access*, Vol. 7, pp. 171023-171031, 2019.

[20] K. Priya and K.K. Rajkumar, "Multiplicative Iterative Nonlinear Constrained Coupled Non-negative Matrix Factorization (MINC-CNMF) for Hyperspectral and Multispectral Image Fusion", *International Journal of Advanced Computer Science and Applications*, Vol. 9, No. 1, pp. 1-23, 2021.

[21] Dataset for Classification, Available at http://lesun.weebly.com/hyperspectral-data-set.html, Accessed at 2021.